# Effect of carotenoid structure on excited-state dynamics of carbonyl carotenoids

**ARTICLE** *in* PHYSICAL CHEMISTRY CHEMICAL PHYSICS · OCTOBER 2009

Impact Factor: 4.49 · DOI: 10.1039/b909924g · Source: PubMed



**4 AUTHORS:**

Pavel Chabera
Lund University
**39** PUBLICATIONS **752** CITATIONS
SEE PROFILE

Marcel Fuciman
University of South Bohemia in České Bud…
**28** PUBLICATIONS **350** CITATIONS
SEE PROFILE

Petr Hribek
Institute of Physics ASCR
**25** PUBLICATIONS **286** CITATIONS
SEE PROFILE

Tomás Polívka
University of South Bohemia in České Bud…
**113** PUBLICATIONS **4,099** CITATIONS
SEE PROFILE

# Effect of carotenoid structure on excited-state dynamics of carbonyl carotenoids

**Pavel Chábera,[a] Marcel Fuciman,[a] Petr Hříbek[a] and Tomáš Polívka*[ab]**

***Received 19th May 2009, Accepted 22nd June 2009***
***First published as an Advance Article on the web 31st July 2009***
**DOI: 10.1039/b909924g**

Effects of introducing a carbonyl group and its position in the conjugated system of carotenoids were studied by means of femtosecond time-resolved spectroscopy. We have compared four naturally occurring carotenoids with comparable structures, β-carotene, echinenone, canthaxanthin and rhodoxanthin, which differ in the number and position of conjugated carbonyl group(s). The $S_1$ lifetime is systematically shorter upon increasing the number of the conjugated C═O groups, yielding 9.3 ps (for β-carotene, no C═O group), 6.2 ps (echinenone, one C═O group), 4.5 ps (canthaxanthin, two C═O groups), and 1.1 ps (rhodoxanthin, two C═O groups in s-*trans* configuration). Except for slight polarity-induced broadening of absorption and transient absorption spectra, no other polarity effects, such as shortening of the $S_1$ lifetimes or transient features attributable to intramolecular charge transfer (ICT) state bands, were observed. The absence of these polarity-induced features is explained as due to the long conjugated chain (no lifetime shortening), and the symmetrical position of the carbonyl groups (no ICT bands). On the other hand, all carotenoids exhibit the characteristic spectral band attributed to the S* state, and for the two longest carotenoids, canthaxanthin and rhodoxanthin, decay of the S* state is markedly longer than that of the $S_1$ state. Moreover, it is shown that the S* state is preferentially populated for a specific subset of ground state conformations, underlining the importance of carotenoid conformation in S* state formation.

## 1. Introduction

Carotenoids with a conjugated carbonyl group are the most abundant in nature. They are synthesized by a variety of plants and microorganisms, but the most studied function of carbonyl carotenoids is light-harvesting in certain groups of marine algae,[1] in which carotenoid-to-chlorophyll energy transfer efficiency approaches in many cases nearly 100%.[1–3] Carbonyl carotenoids have also been successfully used in artificial light-harvesting systems, in which their specific properties allowed the tuning of energy transfer efficiency by solvent polarity.[4] To understand the light-harvesting function, a detailed knowledge of excited-state properties is a key prerequisite. As for their non-carbonyl counterparts, the excited-state properties of carbonyl carotenoids are derived from the idealized $C_{2h}$ symmetry of their conjugated chain. Consequently, the transition from the ground ($S_0$) to the lowest excited-state ($S_1$) is symmetry forbidden as both states are of $A_g^-$ symmetry, and the lowest absorbing state is the $S_2$ ($B_u^+$), making the $S_0$–$S_2$ transition responsible for the strong absorption in the 400–550 nm spectral region. Introduction of the carbonyl group into the conjugated chain causes significant changes in the excited-state properties. The range of effects extends from narrowing of the $S_2$–$S_1$ gap,[5] polarity-induced loss of vibrational structure of the $S_0$–$S_2$ transition that is usually accompanied by asymmetrical broadening towards lower energies, to the polarity-induced shortening of the lowest excited-state lifetime.[5,6] These polarity-induced changes are due to an intramolecular charge transfer (ICT) state whose presence in the excited-state manifold is induced by the conjugated carbonyl group.[5–8]

It is now well established that the ICT state is a key for description of specific photophysics of carbonyl carotenoids, but its coupling to the $S_1$ state is still a matter of a considerable debate.[9] Even though both $S_1$ and ICT states have clearly defined spectral features in transient absorption spectra,[5,6,10] in all experiments carried out so far both $S_1$-like and ICT-like spectral bands decay with identical lifetimes.[5–7,11] In order to explain these results a few models were invoked involving either a strongly coupled $S_1$–ICT system,[5,8] the $S_1$ state itself being the ICT state,[12] or two separate states in thermal equilibrium that makes their lifetimes virtually identical.[13,14] Moreover, a charge transfer character was also observed recently for the $S_2$ state.[15]

The effect of the ICT state on excited-state properties was extensively studied for the highly substituted carotenoid peridinin. Until recently, peridinin was the carotenoid with largest polarity-induced effects; its $S_1$–ICT lifetime varies from 160 to 9 ps when dissolved in non-polar and polar solvents, respectively.[6,10] Recently, however, an even larger effect was observed for the synthetic apocarotenoid 12′-apo-β-carotenal that exhibits all characteristic polarity-induced effects and the $S_1$–ICT lifetime is shortened from 220 ps in *n*-hexane to 8 ps in methanol.[16] An even larger polarity-induced effect has been found in a synthetic peridinin homologue that has a shorter

[a] *Institute of Physical Biology, University of South Bohemia, Zamek 136, 373 33 Nove Hrady, Czech Republic. E-mail: polivka@ufb.jcu.cz*
[b] *Institute of Plant Molecular Biology, Biological Centre, Czech Academy of Sciences, Ceske Budejovice, Czech Republic*

conjugation length than the natural peridinin. The lifetime of 1.5 ns obtained in *n*-hexane was shortened to 9.5 ps in the polar solvent methanol,[17] suggesting that the magnitude of the polarity effect increases with shortening the conjugation length. A number of other carbonyl carotenoids have been studied. Weaker polarity-induced effects observed in other carbonyl carotenoids clearly demonstrated that the position of the conjugated carbonyl group with respect to the main conjugated backbone is important in determining the magnitude of the polarity-induced changes.[5,6] However, no systematic study relating to the position of the carbonyl group has been performed and the relationship between the polarity effect and the position of a carbonyl group remains unclear.

Besides the ICT state, a lot of attention has been devoted to another excited state, the so-called S* state, that was discovered a few years ago in spirilloxanthin. Gradinaru *et al.*[18] showed that the $S_1$–$S_n$ band of spirilloxanthin peaking at $\sim$590 nm has a distinct shoulder at $\sim$540 nm whose lifetime is significantly longer than that of the $S_1$ state (6 ps *vs.* 1.4 ps). Since its discovery, the S* state has been detected in a number of carotenoids. Yet, similarly to the ICT state, the origin and properties of the S* state are ambiguous. While the initial studies did not observe any $S_1$–S* relaxation and both states were assumed to independently decay to the ground state,[9] the recent study by Berera *et al.*[19] clearly showed that a fraction of the S* population may decay to the $S_1$ state. The same S*–$S_1$ relaxation was also observed for non-carbonyl carotenoids at low temperature.[20] These studies consequently place the S* above the $S_1$ state, contrasting the hypothesis proposed by Wohlleben *et al.*, who, based on pump–dump–probe experiments, assigned the S* state to a hot ground state populated by impulsive Raman scattering.[21,22] Moreover, a set of studies by Frank *et al.* provided evidence that the S* state is associated with a twisted molecular conformation of the carotenoid molecule in the $S_1$ state.[20,23,24]

Here we present results of a femtosecond time-resolved absorption study of four carbonyl carotenoids with comparable structures, aiming to understand the relationship between carotenoid structure and behaviour of both ICT and S* states. The four carotenoids chosen for this study, β-carotene, echinenone, canthaxanthin and rhodoxanthin, are shown in Fig. 1. β-Carotene has a well-documented light-harvesting function in the photosynthetic antennae of plants.[25] Echinenone is present in photosynthetic proteins of algae and cyanobacteria,[26,27] but its role in energy transfer has not been established so far. Canthaxanthin occurs predominantly in crustaceans, but also in bacteria, algae and in bird feathers.[27] Rhodoxanthin is a carotenoid with major occurrence in the fruit of the yew tree (*Taxus baccata*).[27] These carotenoids differ by the number and position of the conjugated carbonyl group(s). β-Carotene has no conjugated carbonyl group whereas echinenone contains one, and canthaxanthin two conjugated C═O groups added to the β-ionone rings of β-carotene. Rhodoxanthin also has two conjugated carbonyl groups on the terminal rings, but because it belongs to the family of retro-carotenoids ('retro' indicates a shift of all single and double bonds of the conjugated polyene system by one position[28]), the conjugated carbonyl groups are in s-*trans* orientation with respect to the main conjugated backbone (Fig. 1).

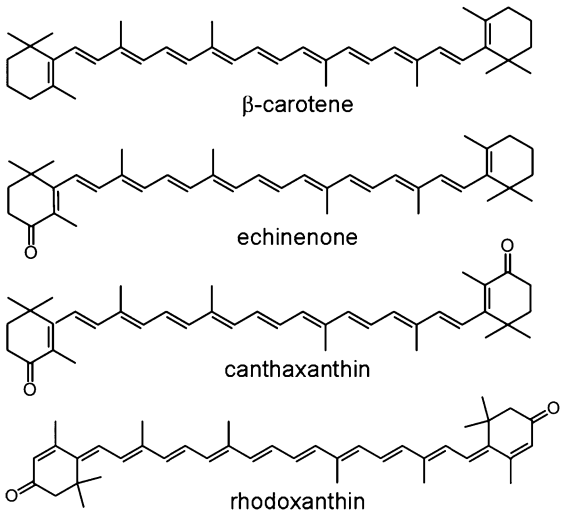


**Fig. 1** Structures of β-carotene, echinenone, canthaxanthin and rhodoxanthin.

## 2. Materials and methods

### Sample preparation

Echinenone, canthaxanthin and rhodoxanthin were purchased from Carotenature (Basel, Switzerland), and β-carotene from Sigma-Aldrich. All carotenoids were used without further purification and stored in the dark at −80 °C. Before experiments, samples were dissolved in dimethyl sulfoxide (DMSO) and benzene to yield an optical density of approximately 0.5 $mm^{-1}$ at the absorption maximum. Absorption spectra were measured in a 1 mm quartz cuvette in a Perkin Elmer Lambda 35 absorption spectrometer with 0.5 nm resolution.

### Time-resolved spectroscopy

The femtosecond spectrometer used for collecting transient absorption spectra is based on a laser system Integra-i (Quantronix). It consists of an Er-fiber oscillator and Ti:Sapphire amplifier producing $\sim$130 fs pulses at a repetition rate of 1 kHz. The central wavelength of the output pulses is 795 nm with an energy per pulse of 2.1 mJ. The amplified pulses were divided into two paths. The first one was directed to the optical parametric amplifier TOPAS to generate tunable excitation pulses, and the second one to produce white-light continuum probe pulses in a 3 mm sapphire plate. The white-light pulses were further divided into the probe beam that overlapped with the pump beam at the sample, and a reference beam. The probe and the reference beams were brought to the slit of a spectrograph where they were dispersed onto a double photodiode array with 1024 elements allowing measurements of transient spectra in a spectral window of $\sim$240 nm. During all measurements, we kept the number of photons per pulse per $cm^2$ under $10^{15}$ to give a reasonable signal to noise ratio but to keep samples without degradation. That there is no contribution from non-linear effects has been verified by increasing the excitation intensity by an order of a magnitude. No changes in transient absorption spectra were observed. In all measurements the mutual polarization of

 

pump and probe beams was set to the magic angle (54.7°) by placing a polarization rotator in the pump beam. All measurements were carried out in a rotational cuvette consisting of two 1 mm quartz windows separated by a 1 mm Teflon spacer.

## 3. Results

### Steady state absorption

The absorption spectra of β-carotene, echinenone, canthaxanthin and rhodoxanthin are shown in Fig. 2. The absorption spectra exhibit a red shift with increasing number of conjugated carbonyl group(s), reflecting the increase in conjugation length. In the non-polar solvent benzene, the maximum of the $S_0$–$S_2$ transition peaks at 465 nm for β-carotene, but addition of a carbonyl group in echinenone shifts the absorption maximum to 472 nm. A further shift to 482 nm is observed for canthaxanthin, which has two carbonyl groups in s-*cis* orientations at both sides of the conjugated backbone (Fig. 1). For rhodoxanthin, the absorption maximum is most red shifted, peaking at 503 nm, revealing the importance of the orientation of the carbonyl group with respect to the main conjugated chain; rhodoxanthin has two carbonyl groups in s-*trans* positions, making the effective conjugation even longer than for canthaxanthin (see Discussion for details). Comparable shifts also occur in the polar solvent DMSO, in which the maximum of the $S_0$–$S_2$ transition occurs at 460 nm (β-carotene), 476 nm (echinenone), 490 nm (canthaxanthin), and 514 nm (rhodoxanthin). When comparing absorption spectra of the same carotenoid in different solvents, it is obvious that the spectra are slightly red shifted and broadened toward lower energies in polar solvents (see Fig. 2 and Table 1).

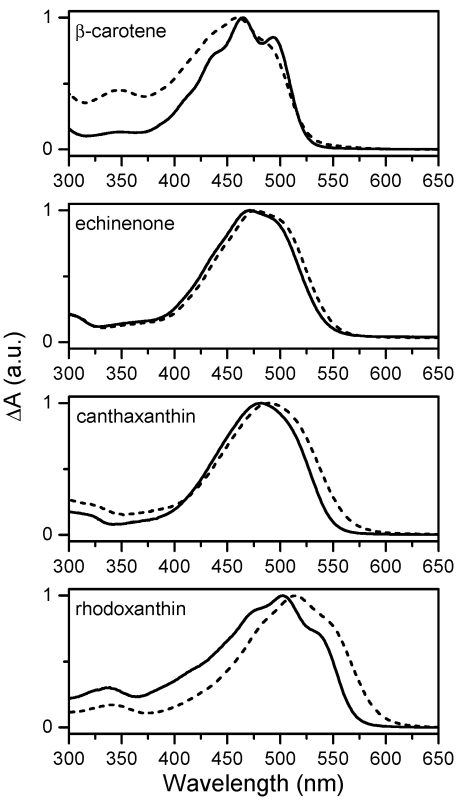


**Fig. 2** Absorption spectra of β-carotene, echinenone, canthaxanthin and rhodoxanthin in DMSO (dashed lines) and benzene (solid lines). All spectra are normalized to the absorption maximum.

It should be noted that benzene and DMSO have nearly identical indices of refraction, 1.50 and 1.48, respectively, thus the shifts are not caused by different polarizabilities. The magnitude of the shift and broadening increases with the number of the conjugated carbonyl groups, which is indicative of polarity-induced effects observed earlier for other carbonyl carotenoids.[5–7] For β-carotene, which lacks the conjugated carbonyl group, no polarity-induced red shift is observed, but an additional peak at 350 nm suggests that isomerization could occur when β-carotene is dissolved in DMSO. A small polarity-induced red shift is observed for echinenone (180 $cm^{-1}$) and a slight asymmetric broadening suggests a weak effect of polarity due to the single conjugated carbonyl group. The largest effect is observed for the two carotenoids with two conjugated carbonyls, canthaxanthin and rhodoxanthin, which exhibit shifts of $\sim$340 $cm^{-1}$ and $\sim$425 $cm^{-1}$, respectively (Table 1). It is worth noting that the polarity-induced red shift of the absorption spectrum for rhodoxanthin is higher than in the case of canthaxanthin, both of which contain two conjugated carbonyl groups. Thus, the difference is invoked by different orientations of the carbonyl groups in the carotenoid molecules. The s-*trans* orientation obviously induces a larger polarity effect. The origin of the interactions causing these polarity-induced shifts is not well understood, but a recent study by Chen *et al.*[29] showed that the difference in absorption maxima in polar and non-polar solvents with comparable polarizabilities is larger for carbonyl carotenoids. Consequently, the polarity-induced shift is likely caused by interaction of the solvent molecules with the carbonyl group. This stabilizes the negative charge at the carbonyl oxygen, decreasing further the $S_2$ energy. Another characteristic polarity-induced change, a loss of vibronic structure of the $S_0$–$S_2$ transition,[5–7] is only marginal for the set of carotenoids studied here. It is mainly because the carotenoids have terminal rings that cause loss of vibronic structure resulting from a conformational disorder in the ground state.[30] It is apparent from Fig. 2 that adding a carbonyl group to the terminal ring further enhances this conformational disorder. In both solvents, β-carotene retains the vibrational structure of the $S_2$ state, but it smears into a hardly distinguished shoulder in echinenone, and to a complete loss of any vibrational structure in canthaxanthin. Interestingly, the vibronic structure is restored for rhodoxanthin, indicating that the linear conjugated chain reduces the distribution of conformers even when the terminal rings are present. The vibrational structure of the rhodoxanthin $S_2$ state is diminished in the polar solvent DMSO, but the polarity-induced loss of vibronic structure is much less than for the carbonyl carotenoids studied earlier.[5–7]

### Transient absorption

The polarity-induced red shifts are further manifested in transient absorption spectra. The transient absorption spectra of all carotenoids recorded at 1 ps after excitation into

**Table 1** Excited-state parameters of carotenoids

| | | | | | | $S_1$–$S_n$ | | $S^*$–$S_N$ | | $S_0$–$S_2$ (max) | |
|---|---|---|---|---|---|---|---|---|---|---|---|
| | Conjugation[a] | Solvent | $\tau_{S_1}$[b]/ps | $\tau_{S^*}$[b]/ps | $\lambda_{exc}$/nm | (nm) | ($cm^{-1}$) | (nm) | ($cm^{-1}$) | (nm) | ($cm^{-1}$) |
| β-Carotene | 9β2 | Benzene | 9.3 | N/A | 500 | 575 | 17 391 | 530 | 18 868 | 465 | 21 505 |
| | | DMSO | 9.7 | N/A | 500 | 576 | 17 361 | 532 | 18 797 | 460 | 21 739 |
| Echinenone | 9β2O | Benzene | 6.2 | N/A | 500 | 607 | 16 474 | 550 | 18 182 | 472 | 21 186 |
| | | DMSO | 6.4 | N/A | 515 | 617 | 16 207 | 565 | 17 699 | 476 | 21 008 |
| Canthaxanthin | 9β2O2 (s-*cis*) | Benzene | 4.5 | 9.1 | 515 | 620 | 16 129 | 556 | 17 986 | 482 | 20 747 |
| | | DMSO | 4.9 | 9.1 | 520 | 628 | 15 924 | 566 | 17 668 | 490 | 20 408 |
| Rhodoxanthin | 12O2 (s-*trans*) | Benzene | 1.1 | 5.6 | 545 | 642 | 15 576 | 575 | 17 391 | 503 | 19 881 |
| | | DMSO | 1.2 | 4 | 550 | 658 | 15 198 | 598 | 16 722 | 514 | 19 455 |

[a] Conjugation length is denoted according to the notation used in ref. 9. *nβmOp* means that the carotenoid has *n* linear conjugated C=C bonds, *m* C=C bonds located at the terminal rings, and *p* conjugated carbonyl groups at the terminal rings. [b] Lifetimes of the $S_1$ and S* states obtained from global fitting analysis. The errors in determining the time constants do not exceed 15%. N/A means that no separate time constant for the S* state has been identified and the $S_1$ and S* bands decay with identical time constant.

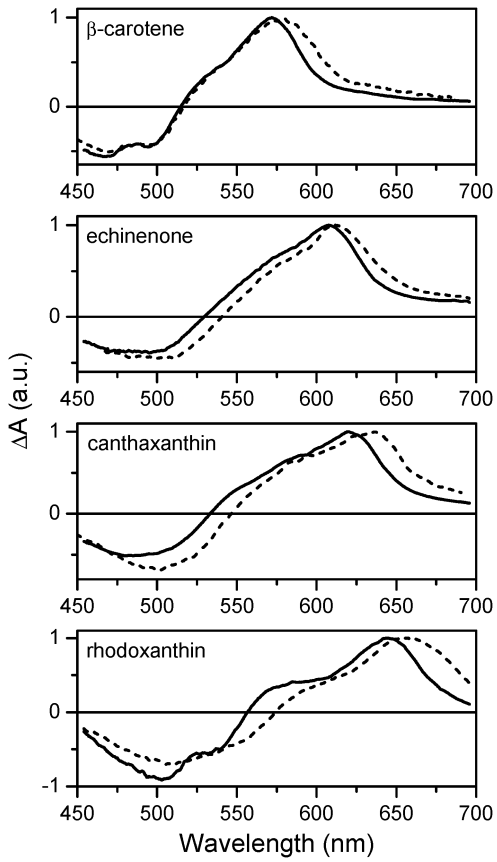


**Fig. 3** Transient absorption spectra of β-carotene, echinenone, canthaxanthin and rhodoxanthin in DMSO (dashed lines) and benzene (solid lines). Transient spectra were recorded at 1 ps after excitation. The wavelengths for excitation were chosen to excite the lowest vibrational band of the $S_2$ state (see Table 1). All spectra are normalized to the maximum.

the 0–0 band of the $S_2$ state are shown in Fig. 3. The spectra consist of two main features, the ground state bleaching mirroring the absorption spectrum and the broad excited-state absorption (ESA) due to the $S_1$–$S_n$ transition.[9] Similarly to the steady-state absorption spectra, the maximum of the $S_1$–$S_n$ band is red shifted as the number of conjugated carbonyl groups increases. In benzene, the $S_1$–$S_n$ band of β-carotene peaks at 575 nm, but a red shift to 607 nm occurs for echinenone, which has one carbonyl group added to the conjugated system. A further red shift to 620 nm is observed for canthaxanthin, having two conjugated carbonyl groups, and the largest shift is found for rhodoxanthin whose $S_1$–$S_n$ band has a maximum at 642 nm. The same trend is observed in DMSO, but the magnitude of the red shift is systematically larger than in the non-polar solvent benzene (Table 1).

The effect of polarity is also demonstrated by the presence of asymmetrical broadening of the $S_1$–$S_n$ band. It is obvious that the intensity of the low-energy part of the $S_1$–$S_n$ band increases with the solvent polarity. Similar behaviour, though for a different pair of solvents, has been observed for other carbonyl carotenoids with comparable structures of the conjugated backbone such as hydroxyechinenone,[31] astaxanthin,[32] or salinixanthin.[33] Contrary to other carbonyl carotenoids, for which the increase in polarity causes formation of a new spectral band attributed to the ICT state,[5–7,15] the mild asymmetrical broadening of the $S_1$–$S_n$ band observed here rather reflects a broader distribution of excited-state conformers, indicating that the role of the ICT state is likely negligible in carbonyl carotenoids with the conjugated carbonyl group located at the terminal ring (see Discussion section).

Kinetics recorded at the maximum of the $S_1$–$S_n$ transient absorption band (Fig. 4) show the trend of the shortening of the $S_1$ lifetime with increasing number of conjugated carbonyl groups which reflects prolongation of the conjugation length. Adding one carbonyl group to the conjugated system of β-carotene shortens the $S_1$ lifetime from ~9 ps to ~6 ps (echinenone). The $S_1$ lifetime is further shortened to ~4.5 ps (in canthaxanthin), and the $S_1$ lifetime of ~1.1 ps is observed in rhodoxanthin. Essentially the same trend is observed in DMSO, in which the lifetimes are, within experimental error, identical with those in benzene (Table 1). This further underlines the absence of any significant effects of the ICT state in these carotenoids, as it is known that for carotenoids with shorter conjugation length the presence of ICT induces shortening of the $S_1$ lifetime upon increase of the solvent polarity.[5,6,34]

Another important feature in all transient spectra is a distinct shoulder observed at the high-energy part of the $S_1$–$S_n$ ESA band. This shoulder is usually ascribed to the so-called S* state.[18,35] The $S^*$–$S_N$ transition band is most

 

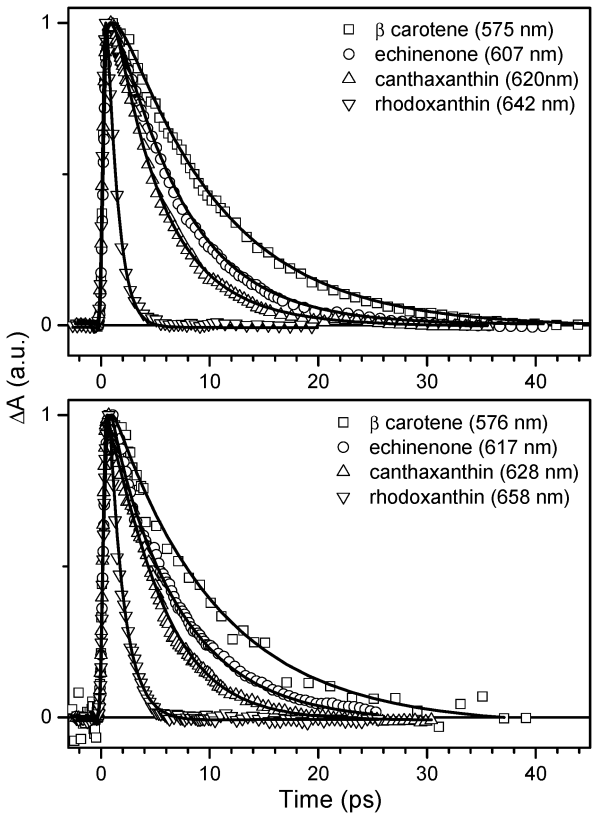


**Fig. 4** Kinetics measured at the maximum of the $S_1$–$S_n$ band after excitation to the lowest vibrational band of $S_2$ state. Kinetics were measured in benzene (top) and DMSO (bottom). The solid lines correspond to the fitting of kinetics data. Probing wavelengths are in parentheses, and excitation wavelengths are summarized in Table 1.

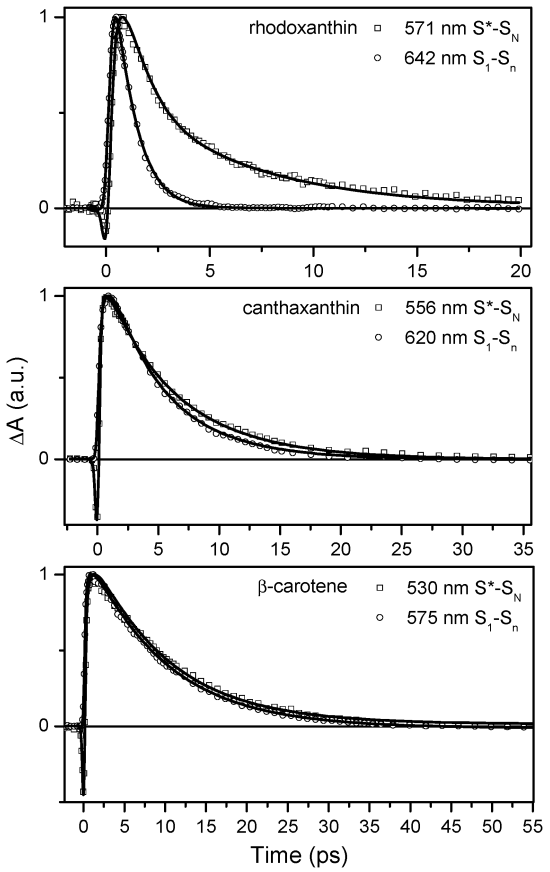


**Fig. 5** Kinetics of rhodoxanthin, canthaxanthin and β-carotene recorded at the maximum of the S* (squares) and $S_1$ bands (circles) in benzene. The solid lines correspond to the fitting of kinetics data. For excitation wavelengths see Table 1.

pronounced for rhodoxanthin, and a clear shoulder is also identified in β-carotene (Fig. 3). In echinenone and canthaxanthin, only a hint of a shoulder attributable to the S*–$S_N$ transition can be observed, but kinetics measured in the spectral region where the S*–$S_N$ band is expected show differences from those measured at the maximum of the $S_1$–$S_n$ band (see below). Changing solvent from benzene to DMSO does not affect the magnitude of the S* band, but its position is red shifted in DMSO, following the red shift of the $S_1$–$S_n$ band. Spectral positions of the ESA bands for all carotenoids in both solvents are summarized in Table 1. When comparing the kinetics measured at the maxima of the $S_1$–$S_n$ and S*–$S_N$ bands, it is obvious that there are some differences. A common difference is the presence of negative signal around time zero in the S*–$S_N$ kinetics that is due to the stimulated emission from the $S_2$ state that extends far beyond 500 nm. Differences at longer delays are especially pronounced for rhodoxanthin, where the S* band cannot be fitted by a single-exponential function and requires an additional component to fit the longer decay component that is not required when fitting the $S_1$ decay (Fig. 5). In benzene, the $S_1$ state decays with a time constant of ~1 ps, but fitting the S* band requires an additional component of 5.6 ps. The same situation occurs in DMSO, although the additional time component due to the S* state is slightly shorter, yielding 4 ps (see Table 1). A similar effect is observed for canthaxanthin, whose $S_1$ state has a 4.5 ps lifetime in benzene, but an additional time component of 9.1 ps characterizing the S* decay is required to fit the kinetics measured in the spectral region of the S*–$S_N$ transition. No additional time components were necessary to fit the kinetics of β-carotene (Fig. 5) and echinenone measured at the maxima of the $S_1$–$S_n$ and S*–$S_N$ bands.

## Global fitting

Further insight into the excited-state dynamics is achieved by global fitting of all kinetics simultaneously to a sum of exponentials. For simplicity, we used a model with time evolution according to a sequential, irreversible scheme A → B, B → C.... The arrows represent increasingly slower monoexponential processes and the time constants of these processes correspond to lifetimes of the species A, B, C.... The spectral profiles of the species are called evolution-associated difference spectra (EADS). Although in complex systems EADS do not necessarily correspond to difference absorption spectra of particular excited states, they help to visualize the excited-state dynamics.[36]

The EADS obtained from global analysis are depicted in Fig. 6 for rhodoxanthin and canthaxanthin in benzene. The first EADS (solid lines) represent spectra of the initially excited $S_2$ states of rhodoxanthin and canthaxanthin. They consist of the ground state bleaching and stimulated emission (SE)

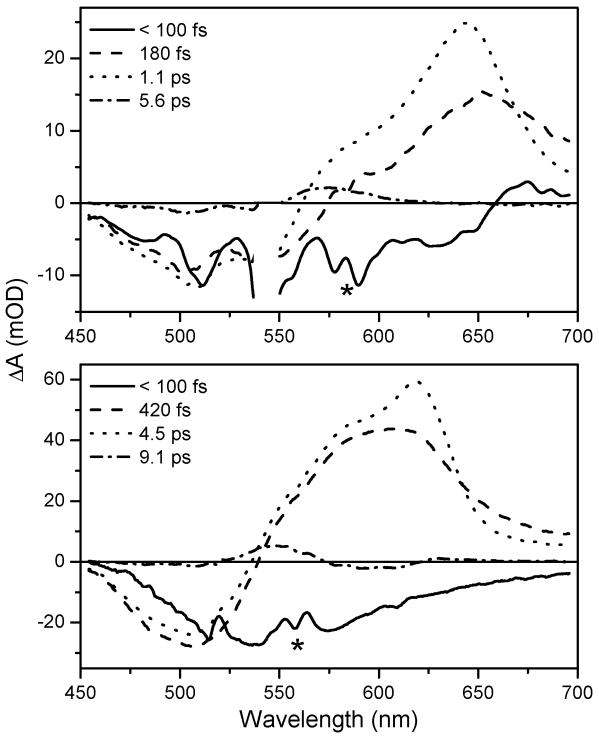


**Fig. 6** EADS obtained from global fitting of rhodoxanthin (top) and canthaxanthin (bottom) in benzene. See text for details.

from the $S_2$ state. The first EADS also contain clearly distinguishable Raman peaks (marked by asterisks in Fig. 6) whose energy gaps from excitation are 1180 and 1550 $cm^{-1}$, matching the frequencies of the ground state C–C and C═C stretches, respectively. This first EADS decays in both rhodoxanthin and canthaxanthin in less than 100 fs to form the second EADS (dashed line) which exhibits typical attributes of a hot $S_1$ state.[24,37] The EADS of the hot $S_1$ state decays within ~180 fs in rhodoxanthin and ~420 fs in canthaxanthin to produce a characteristic spectrum of the thermally relaxed $S_1$ state (dotted lines). Besides the $S_1$–$S_n$ transition, peaking at 642 nm and 620 nm in rhodoxanthin and canthaxanthin, respectively, a distinct shoulder at the blue side of the $S_1$–$S_n$ band indicates mixing of the S* band into the pure $S_1$–$S_n$ spectrum. However, a pure spectrum of the S* state is obtained in the final EADS that forms within ~1.1 ps in rhodoxanthin and ~4.5 ps in canthaxanthin. This final EADS decays with a lifetime of 5.6 ps (rhodoxanthin) and 9.1 ps (canthaxanthin). For β-carotene and echinenone, no separate lifetime of the S* state has been identified. The lifetimes of the decay components obtained from global fitting are summarized in Table 1.

## 4. Discussion

### Effective conjugation length

In order to evaluate effects of the presence and position of the conjugated carbonyl group on excited-state properties of the studied carotenoids, we begin with a question: how the conjugated carbonyl group affects the effective conjugation length, $N_{eff}$. Since the $S_1$ lifetime of non-carbonyl carotenoids follows the energy gap law,[38] $N_{eff}$ of a carotenoid with various functional groups is usually estimated on the basis of comparison of its $S_1$ lifetime with the lifetimes of carotenoids with linear conjugated chain. Thus, the $S_1$ lifetime of β-carotene of ~9.5 ps, which has 9 linear C═C bonds and two conjugated C═C bonds in s-*cis* orientation located at the terminal rings, is comparable to the $S_1$ lifetime of the linear carotenoid spheroidene which has 10 conjugated C═C bonds.[39] Consequently, we can estimate $N_{eff} \approx 10$ for β-carotene, indicating that each of the two C═C bonds in s-*cis* orientation contributes by 0.5 to the total conjugation length. The same approach can be applied for echinenone, canthaxanthin and rhodoxanthin. Although these carotenoids have their conjugation extended to the carbonyl group which is known to modify the $S_1$ lifetimes in polar environment, no significant polarity effect on $S_1$ lifetime has been observed for the carotenoids studied here, and this complication can be neglected. The $S_1$ lifetimes obtained from global fitting yield values of ~6 ps (echinenone), ~4.5 ps (canthaxanthin), and ~1 ps (rhodoxanthin). Comparing these $S_1$ lifetimes with known lifetimes of linear carotenoids (see *e.g.* Table 3 in ref. 9), we obtain values of $N_{eff} \approx 10.5$ for echinenone, $N_{eff} \approx 11$ for canthaxanthin, and $N_{eff} \approx 13$ for rhodoxanthin. Thus, it can be concluded that regardless of the position, the conjugation extended to a carbonyl group always adds 0.5 to $N_{eff}$, while for a C═C group located at a terminal ring it is important whether it is in s-*cis* (contributing by 0.5 to $N_{eff}$) or s-*trans* (contributing by 1 to $N_{eff}$) orientation.

### Effects of the carbonyl group

Having established the effect of the carbonyl groups on the effective conjugation length, we may now turn to evaluation of the influence of the conjugated carbonyl groups on the excited-state properties. A minor effect can be traced in the absorption spectra which exhibit a small red shift upon change of solvent polarity. Since benzene and DMSO have essentially equal polarizabilities, the red shift in DMSO cannot be attributed to the well-known stabilization of the $S_2$ energy in highly-polarizable solvents.[40] Moreover, the magnitude of the red shift clearly depends on the number and position of the conjugated carbonyl group(s). A polarity-induced red shift of ~180 $cm^{-1}$ occurs for echinenone, larger red shift of ~340 $cm^{-1}$ is observed for canthaxanthin, and the largest solvent-induced red shift of ~425 $cm^{-1}$ is found in rhodoxanthin. Thus, it is clear that the presence of the conjugated carbonyl group shifts the $S_2$ state to lower energy in polar solvents, in agreement with earlier observations on other carbonyl carotenoids.[5]

Polarity-induced red shifts of a comparable magnitude are also observed in transient absorption spectra. In addition to the red shift, however, the carotenoids containing conjugated carbonyl group(s) exhibit asymmetric broadening of the $S_1$–$S_n$ transition towards lower energies (Fig. 3). A similar effect was also observed for other carbonyl carotenoids with $N_{eff} > 10$, such as hydroxyechinenone,[31] salinixanthin[33] or adonixanthin.[41] This broadening is attributed to a broader distribution of conformers induced by the presence of the ICT state, but except for the broadening, no ICT-specific bands, which were identified for a number of carbonyl carotenoids with shorter

 

conjugation,[5–7] have been observed here. Although the absence of specific ICT bands fits into the generally accepted scheme of the ICT state having a negligible effect on the excited-state properties of carotenoids with $N_{eff} > 10$, it should be noted that the ICT bands in transient absorption spectra were observed in spheroidenone, which has $N_{eff} \approx 10.5$.[5,6] Thus, it is obvious that merely the conjugation length dependence cannot explain the observed data, and other factors must be taken into account. Comparison of the structures of spheroidenone, which has a conjugated chain consisting of 10 linear C=C bonds and one C=O bond in s-*cis* orientation attached directly to the linear C=C backbone,[5,6] with those of carotenoids studied here (Fig. 1) indicates that asymmetry in the position of the carbonyl group(s) is likely the key property to observe the ICT bands. While both rhodoxanthin and canthaxanthin have two carbonyl groups arranged symmetrically with respect to the main conjugated backbone, the single carbonyl group of spheroidenone introduces asymmetry into the conjugated chain that is responsible for the ICT-specific transient absorption bands. It may be argued that the same asymmetry also exists in echinenone (Fig. 1), but it seems that isolation of the conjugated carbonyl group at the terminal ring, which is twisted with respect to the main conjugation,[30] prevents observation of the ICT-specific bands. This hypothesis is further supported by experiments on hydroxyechinenone, which has an identical structure of the conjugated chain to that of echinenone, but has an extra hydroxyl group at the terminal ring. It was shown that while in solution there are no ICT-specific bands in the transient absorption spectra regardless of the solvent polarity, the ICT band is induced upon binding to protein which forces the terminal ring containing the carbonyl group to twist, making the conjugated chain linear with a single conjugated carbonyl group at the end.[31]

The absence of any polarity-induced shortening of the $S_1$ lifetime is in accordance with previous results, further underlining the fact that this effect can be observed only for carotenoids with $S_1$ lifetimes longer than $\sim$10 ps in non-polar solvents. For a number of carbonyl carotenoids it has been observed that, regardless of the molecular structure, the shortest $S_1$ lifetimes measured in the most polar solvents converge to 8–10 ps even though their $S_1$ lifetimes in a non-polar solvent differ significantly.[6,7,11,17] Thus, it seems that the polarity-induced stabilization of the ICT state of carbonyl carotenoids, which leads to the lifetime shortening, cannot make the $S_1$ state shorter than $\sim$10 ps. Thus, all carbonyl carotenoids with $S_1$ lifetimes shorter than 10 ps do not experience the shortening of the $S_1$ lifetime in polar solvents. This means that while the lifetime shortening is determined by the energy of the ICT state, the presence of the ICT-bands in the transient absorption spectrum is related to the position of the conjugated carbonyl group with respect to the main conjugated chain, indicating that in order to make the ICT-like transition allowed, a significant asymmetry has to be induced.

### The S* state

Although we have not observed any specific bands in polar solvents attributable to the ICT state, the two longest carotenoids, canthaxanthin and rhodoxanthin, exhibit a clear indication that the S* state is involved in their excited-state dynamics (Fig. 5). The presence of a longer decay component extracted from the global fitting (Fig. 6) has a spectral profile characteristic of the S* state,[18,23,35] but its lifetime differs for the two carotenoids, yielding lifetimes of 5.6 and 9 ps for rhodoxanthin and canthaxanthin in benzene, respectively. The S* lifetime of rhodoxanthin is even shorter in DMSO, 4 ps, which makes it shorter than that of the non-carbonyl carotenoid spirilloxanthin (6 ps) which has comparable effective conjugation length.[18] It is therefore obvious that the carotenoid structure is an important factor in determining the S* decay. It was demonstrated that linear carotenoids have similar S* lifetimes regardless of their conjugation length,[18,21,42] but as pointed out by Niedzwiedzki *et al.*,[23] the S* state gained more population and had a shorter lifetime in carotenoids with conjugation extended to the terminal rings. The shorter S* lifetime of rhodoxanthin as compared with spirilloxanthin is in accordance with this notion; even though the effective conjugation lengths of these carotenoids are similar and both carotenoids have linear conjugated chains, the extension of the conjugation to the terminal rings of rhodoxanthin (Fig. 1) decreases the S* lifetime. This observation supports the conclusion of Niedzwiedzki *et al.*[23,24] that the spectroscopic properties of the S* state are largely determined by the carotenoid structure and not by its conjugation length.[23,24]

To gain more insight into the origin of the S* state, we have analysed the bleaching region of transient absorption spectra. In order to compare the bleaching bands of carotenoids when the dominant population is either in the $S_1$ or S* state, normalized transient spectra taken at two delay times, $\tau_1$ and $\tau_2$, are shown in Fig. 7. The spectrum at time $\tau_1$ is chosen to reflect mainly the $S_1$ state population as it is measured at a delay time when the $S_2$–$S_1$ relaxation is mostly finished, and majority of the excited-state population is in the $S_1$ state. On the other hand, time $\tau_2$ is much longer than the $S_1$ lifetime, thus the spectrum at $\tau_2$ characterizes the S* population. Comparison of the bleaching regions at $\tau_1$ and $\tau_2$ clearly reveals that when the $S_1$ state is populated, the resolution of vibrational bands in the bleaching region matches that of the steady-state absorption spectrum. However, at longer delay times when the S* state gains population, the vibrational bands in the bleaching region are significantly more pronounced. This clearly suggests that the S* population arises from a specific subset of ground state conformers, because if the S* population were determined exclusively by excited-state properties, the bleaching bands should mirror the shape of the steady-state absorption spectrum regardless of the carotenoid is in the S* or $S_1$ state. The effect is strongest in rhodoxanthin, but clearly pronounced also in canthaxanthin as in both the S* spectrum can be reliably separated from the $S_1$ spectrum. Interestingly, however, the effect is observable even in β-carotene, indicating that our minimal model of sequential fitting is not capable of separating the $S_1$ and S* lifetimes, which are very similar in β-carotene. Although the kinetics measured at the $S_1$ maximum and in the S* region are nearly identical (Fig. 5), comparison of the transient absorption spectra unequivocally identifies the S* state also in β-carotene,

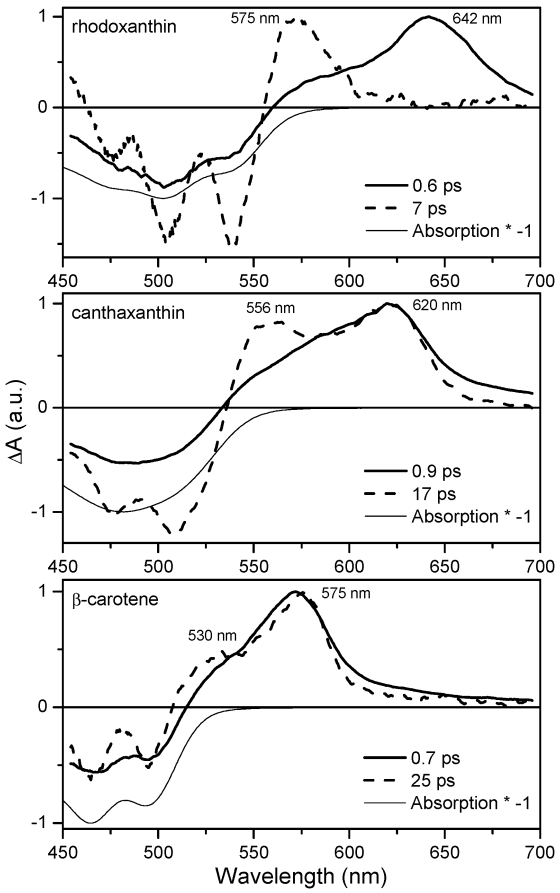


**Fig. 7** Transient absorption spectra of rhodoxanthin, canthaxanthin and β-carotene in benzene at delay times corresponding to the $S_1$ population (thick solid lines) and the S* population (dashed lines). All spectra are normalized to their maxima. The thin solid line represents the inverted absorption spectrum in benzene. Excitation wavelengths are in Table 1.

confirming the results of pump–deplete–probe spectroscopy.[43] The fact that the S* state of β-carotene must have a lifetime very similar to that of the $S_1$ state, *i.e.* ~9.5 ps, again shows that the S* lifetimes do not follow the conjugation length dependence known for the $S_1$ lifetimes; although β-carotene and canthaxanthin have different effective conjugation lengths (10 and 11, respectively) and correspondingly different $S_1$ lifetimes (9.5 and 4.5 ps), their S* lifetimes are nearly the same, 9–9.5 ps.

Thus, our results revive the inhomogeneous model of the S* population, first invoked by Papagiannakis *et al.*,[44] but ruled out on the basis of results showing that the S* and $S_1$ populations have markedly different dependence on excitation intensity.[44,45] Based on the experiments presented here, however, the ground state inhomogeneity has to be taken into account, because our data show that certain ground state conformations have a higher probability of reaching the S* state than others. Given the very good resolution of the vibrational bands it may be expected that it is the population with more planar π-conjugation that slightly favours the route to the S* state. It must be noted, however, that the ground state inhomogeneity alone cannot explain the intensity-dependent behaviour of the S* state population. Instead, some non-linear process must be involved in the S* pathway[44,45] and our results suggest that certain ground state conformations likely enhance the non-linear process directing the molecules to the S* state. Currently, two such processes have been suggested to operate in carotenoids: (1) sequential two-photon absorption that populates higher excited states whose decay predominantly populates the S* state,[44] or (2) the S* state is populated *via* impulsive stimulated Raman scattering.[21,45] While the first process assumes that the S* state is a separate excited state associated with a twisted carotenoid conformation,[23,24,44] the second non-linear process suggests that the S* state could be a hot ground state.[21,45] The results presented here cannot determine the validity of these two models, because none of them can be falsified on the basis of our experiments. Yet, it clearly shows that the ground state inhomogeneity plays an important role, explaining why the S* state population is observed mainly in carotenoids with longer conjugation and it is further enhanced for those having the conjugation extended to terminal rings. These carotenoids have a broader distribution of the ground state conformers, thus enhancing the probability of the excited-state population going to the S* state.

## Acknowledgements

Research was supported by grants from the Czech Ministry of Education (MSM6007665808 and AV0Z50510513), and Grant Agency of the Czech Academy of Sciences (IAA608170604).

## References

1 A. N. Macpherson and R. G. Hiller, in *Photochemistry of Carotenoids*, ed. B. R. Green and W. W. Parson, Kluwer Academic Publishers, Dordrecht, Netherlands, 2003, pp. 323–352.
2 J. A. Bautista, R. G. Hiller, F. P. Sharples, D. Gosztola, M. Wasielewski and H. A. Frank, *J. Phys. Chem. A*, 1999, **103**, 2267–2273.
3 T. Polívka, R. G. Hiller and H. A. Frank, *Arch. Biochem. Biophys.*, 2007, **458**, 111–120.
4 T. Polívka, M. Pellnor, E. Melo, T. Pascher, V. Sundström, A. Osuka and K. R. Naqvi, *J. Phys. Chem. C*, 2007, **111**, 467–476.
5 D. Zigmantas, R. G. Hiller, F. P. Sharples, H. A. Frank, V. Sundström and T. Polívka, *Phys. Chem. Chem. Phys.*, 2004, **6**, 3009–3016.
6 H. A. Frank, J. A. Bautista, J. Josue, Z. Pendon, R. G. Hiller, F. P. Sharples, D. Gosztola and M. R. Wasielewski, *J. Phys. Chem. B*, 2000, **104**, 4569–4577.
7 S. Stalke, D. A. Wild, T. Lenzer, M. Kopczynski, P. W. Lohse and K. Oum, *Phys. Chem. Chem. Phys.*, 2008, **10**, 2180–2188.
8 D. Zigmantas, R. G. Hiller, A. Yartsev, V. Sundström and T. Polívka, *J. Phys. Chem. B*, 2003, **107**, 5339–5348.
9 T. Polivka and V. Sundström, *Chem. Rev.*, 2004, **104**, 2021–2072.
10 D. Zigmantas, T. Polívka, R. G. Hiller, A. Yartsev and V. Sundström, *J. Phys. Chem. A*, 2001, **105**, 10296–10306.
11 N. Chatterjee, D. M. Niedzwiedzki, K. Aoki, T. Kajikawa, S. Katsumura, H. Hashimoto and H. A. Frank, *Arch. Biochem. Biophys.*, 2009, **483**, 146–155.
12 S. Shima, R. P. Ilagan, N. Gillespie, B. J. Sommer, R. G. Hiller, F. P. Sharples, H. A. Frank and R. R. Birge, *J. Phys. Chem. B*, 2003, **107**, 8052–8066.
13 E. Papagiannakis, M. Vengris, D. S. Larsen, I. H. M. van Stokkum, R. G. Hiller and R. van Grondelle, *J. Phys. Chem. B*, 2006, **110**, 512–521.
14 P. A. Linden, J. Zimmermann, T. Brixner, N. E. Holt, H. M. Vaswani, R. G. Hiller and G. R. Fleming, *J. Phys. Chem. B*, 2004, **108**, 10340–10345.

 

15 L. Premvardhan, E. Papagiannakis, R. G. Hiller and R. van Grondelle, *J. Phys. Chem. B*, 2005, **109**, 15589–15597.
16 D. A. Wild, K. Winkler, S. Stalke, K. Oum and T. Lenzer, *Phys. Chem. Chem. Phys.*, 2006, **8**, 2499–2505.
17 N. Chatterjee, D. M. Niedzwiedzki, T. Kajikawa, S. Hasegawa, S. Katsumara and H. A. Frank, *Chem. Phys. Lett.*, 2008, **463**, 219–224.
18 C. C. Gradinaru, J. T. M. Kennis, E. Papagiannakis, I. H. M. van Stokkum, R. J. Cogdell, G. R. Fleming, R. A. Niederman and R. van Grondelle, *Proc. Natl. Acad. Sci. U. S. A.*, 2001, **98**, 2364–2369.
19 R. Berera, I. H. M. van Stokkum, G. Kodis, A. E. Keirstead, S. Pillai, Ch. Herrero, R. E. Palacios, M. Vengris, R. van Grondelle, D. Gust, T. A. Moore, A. L. Moore and J. T. M. Kennis, *J. Phys. Chem. B*, 2007, **111**, 6868–6877.
20 H. Cong, D. M. Niedzwiedzki, G. N. Gibson and H. A. Frank, *J. Phys. Chem. B*, 2008, **112**, 3558–3567.
21 T. Buckup, J. Savolainen, W. Wohlleben, J. L. Herek, H. Hashimoto, R. R. B. Correia and M. Motzkus, *J. Chem. Phys.*, 2006, **125**, 194505.
22 T. Buckup, J. Hauer, J. Mohring and M. Motzkus, *Arch. Biochem. Biophys.*, 2009, **483**, 219–223.
23 D. M. Niedzwiedzki, J. O. Sullivan, T. Polívka, R. R. Birge and H. A. Frank, *J. Phys. Chem. B*, 2006, **110**, 22872–22885.
24 D. M. Niedzwiedzki, J. F. Koscielecki, H. Cong, J. O. Sullivan, G. N. Gibson, R. R. Birge and H. A. Frank, *J. Phys. Chem. B*, 2007, **111**, 5984–5998.
25 J. T. M. Kennis, B. Gobets, I. H. M. van Stokkum, J. P. Dekker, R. van Grondelle and G. R. Fleming, *J. Phys. Chem. B*, 2001, **105**, 4485–4494.
26 R. Berera, I. H. M. van Stokkum, S. d'Haene, J. T. M. Kennis, R. van Grondelle and J. P. Dekker, *Biophys. J.*, 2009, **96**, 2261–2267.
27 *Carotenoids Handbook*, ed. G. Britton, S. Liaaen-Jensen and H. Pfander, Birkhauser Verlag, Basel, Switzerland, 2004.
28 *Carotenoids: Isolation and Analysis*, ed. G. Britton, S. Liaaen-Jensen and H. Pfander, Birkhauser Verlag, Basel, Switzerland, 1995, p 64.
29 Z. Chen, C. Lee, T. Lenzer and K. Oum, *J. Phys. Chem. A*, 2006, **110**, 11291–11297.
30 R. L. Christensen, M. Goyette, L. Gallagher, J. Duncan, B. D. Lugtenburg, F. J. Jansen and I. van der Hoef, *J. Phys. Chem. A*, 1999, **103**, 2399–2407.
31 T. Polívka, C. A. Kerfeld, T. Pascher and V. Sundström, *Biochemistry*, 2005, **44**, 3994–4003.
32 R. P. Ilagan, R. L. Christensen, T. W. Chapp, G. N. Gibson, T. Pascher, T. Polívka and H. A. Frank, *J. Phys. Chem. A*, 2005, **109**, 3120–3127.
33 T. Polívka, S. P. Balashov, P. Chábera, E. S. Imasheva, A. Yartsev, V. Sundström and J. K. Lanyi, *Biophys. J.*, 2009, **96**, 2268–2277.
34 M. Kopczynski, F. Ehlers, T. Lenzer and K. Oum, *J. Phys. Chem. A*, 2007, **111**, 5370–5381.
35 E. Papagiannakis, J. T. M. Kennis, I. H. M. van Stokkum, R. J. Cogdell and R. van Grondelle, *Proc. Natl. Acad. Sci. U. S. A.*, 2002, **99**, 6017–6022.
36 I. H. M. van Stokkum, D. S. Larsen and R. van Grondelle, *Biochim. Biophys. Acta*, 2004, **1657**, 82–104.
37 F. L. de Weerd, I. H. M. van Stokkum and R. van Grondelle, *Chem. Phys. Lett.*, 2002, **354**, 38–43.
38 V. Chynwat and H. A. Frank, *Chem. Phys.*, 1995, **194**, 237–244.
39 T. Polivka, D. Zigmantas, H. A. Frank, J. A. Bautista, J. L. Herek, Y. Koyama, R. Fujii and V. Sundstrom, *J. Phys. Chem. B*, 2001, **105**, 1072–1080.
40 A. N. Macpherson and T. Gillbro, *J. Phys. Chem. A*, 1998, **102**, 5049–5058.
41 T. Lenzer, S. Schubert, F. Ehlers, P. W. Lohse, M. Scholz and K. Oum, *Arch. Biochem. Biophys.*, 2009, **483**, 213–218.
42 W. Wohlleben, T. Buckup, J. L. Herek, R. J. Cogdell and M. Motzkus, *Biophys. J.*, 2003, **85**, 442–450.
43 W. Wohlleben, T. Buckup, H. Hashimoto, R. J. Cogdell, J. L. Herek and M. Motzkus, *J. Phys. Chem. B*, 2004, **108**, 3320–3325.
44 E. Papagiannakis, I. H. M. van Stokkum, M. Vengris, R. J. Cogdell, R. van Grondelle and D. S. Larsen, *J. Phys. Chem. B*, 2006, **110**, 5727–5736.
45 J. Savolainen, T. Buckup, J. Hauer, A. Jafarpour, C. Serrat, M. Motzkus and J. L. Herek, *Chem. Phys.*, 2009, **357**, 181–187.